

Fig. 1. The centrosymmetric $\text{Hg}_2(\text{NO}_2)_2$ complex with atom numbering, bond lengths (Å) and angles ($^\circ$).

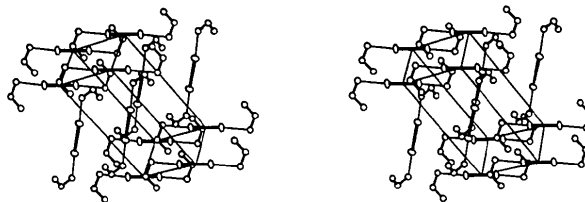


Fig. 2. A stereoscopic view of the structure.

Discussion. The structure of the $\text{Hg}_2(\text{NO}_2)_2$ molecular unit is shown in Fig. 1, which also gives the bond lengths and bond angles. The non-bonded Hg—O distances, $\text{Hg}\cdots\text{O}(2)$ ($x-1, y, z$) = 2.93 (2) and $\text{Hg}\cdots\text{O}(1)$ ($x, -\frac{1}{2}-y, -\frac{1}{2}+z$) = 2.84 (2) Å, suggest some interaction, since the van der Waals radius of oxygen is 1.4 Å and the closest Hg—Hg distance in solid mercury is estimated to be ~ 3.0 Å (Evans, 1978). Similar weak interactions have been noted in $\text{Hg}_2(\text{BrO}_3)_2$ (Dorm, 1967) and in Hg_2SO_4 and Hg_2SeO_4 (Dorm, 1969). The bonded —O—Hg—Hg—O system is approximately linear and the molecular unit is planar (deviations from the best plane are all < 0.01 Å) and centrosymmetric. The N—O bond lengths correspond with that observed, for instance, in sodium nitrite, 1.240 (3) Å (Kay, Frazer & Ueda, 1962).

The crystal packing, illustrated in Fig. 2, shows no special features. The average volume occupied per atom is 17.0 Å³; the $\text{Hg}_2(\text{NO}_2)_2$ molecules pack together in quite a compact way. The Hg atoms are four-coordinated, involving the bonding and non-bonding interactions discussed above.

We thank the University of South Africa and the University Grants Division of the Council for Scientific and Industrial Research for financial support and Dr P. van Rooyen of the National Chemical Research Laboratory for data collection.

References

- DORM, E. (1967). *Acta Chem. Scand.* **21**, 2834–2840.
 DORM, E. (1969). *Acta Chem. Scand.* **23**, 1607–1615.
 EVANS, E. C. (1978). *An Introduction to Crystal Chemistry*, 2nd ed., pp. 87, 112. Cambridge Univ. Press.
 GROTH, P. (1906). *Chemische Krystallographie*, Vol. II, p. 19. Leipzig: Engelmann. Photoreproduction (1959), The Groth Institute, Univ. Park, Pennsylvania.
International Tables for X-ray Crystallography (1974). Vol. IV, pp. 99, 149. Birmingham: Kynoch Press. (Present distributor D. Reidel, Dordrecht.)
 KAY, M. I., FRAZER, B. C. & UEDA, R. (1962). *J. Phys. Soc. Jpn.* **17**, Suppl. B III, 389–391.
 NORTH, A. C. T., PHILLIPS, D. C. & MATHEWS, F. S. (1968). *Acta Cryst.* **A24**, 351–359.
 POTTS, R. A. & ALLRED, A. L. (1966). *Inorg. Chem.* **5**, 1066–1071.
 SHELDRIK, G. M. (1976). *SHELX*. Program for crystal structure determination. Univ. of Cambridge, England.

Acta Cryst. (1985). **C41**, 998–1003

Structure of $\text{Pb}_3\text{O}_2(\text{OH})_2$ by Rietveld Analysis of Neutron Powder Diffraction Data

BY RODERICK J. HILL

CSIRO Division of Mineral Chemistry, PO Box 124, Port Melbourne, Victoria 3207, Australia

(Received 3 December 1984; accepted 6 February 1985)

Abstract. $M_r = 687.58$, tetragonal, $P\bar{4}2_1c$, $a = 8.0226$ (3), $c = 9.3183$ (4) Å, $V = 599.69$ (7) Å³, $Z = 4$, $D_x = 7.619$ g cm⁻³, $\lambda = 1.893$ Å, $\mu = 0.433$ cm⁻¹, $F(000) = 1757$ fm², $T = 295$ K, $R_{wp} = 0.0356$ for 2900 step intensities, $R_B = 0.0116$ for 221 reflections. The structure consists of discrete dodecahedral clusters with composition $\text{Pb}_6\text{O}_4(\text{OH})_4$ and $\bar{4}$ symmetry, fixed in position at the corners and centre of the unit cell by eight hydrogen bonds of length 1.87 (2) Å and by van

der Waals interactions between Pb lone-pair orbitals. The two distinct Pb atoms are square-pyramidally coordinated by two O atoms and two OH groups. Both O atoms are trigonally coordinated by Pb, but are significantly displaced from the plane of these atoms as a result of their bonds to H. Thermal decomposition (essentially complete in the temperature range 410–460 K) and infrared absorption (no structural water) properties are also described.

Introduction. Alkaline solutions of divalent lead have been shown to contain a large number of possible lead-hydroxy complex ions (Abel, 1973), which, in the absence of carbon dioxide, may precipitate out as phases with the general formulation $x\text{PbO}\cdot\text{H}_2\text{O}$, where $x = 1-3$ (Clark & Tyler, 1939; Robin & Théolier, 1956; Tolkachev, Stroganov & Kozina, 1958; Todd & Parry, 1964; Howie & Moser, 1968; Oswald, Gunter & Stahlin, 1968; Glemser & Lin, 1971). It is, however, not always easy to discriminate between these compounds analytically since they can differ by as little as one water molecule per fifteen formula units of PbO and they usually occur as powders with large surface area and poor crystallinity. Moreover, their X-ray powder diffraction patterns are so dominated by scattering from the lead atoms that variations in the arrangement of the oxygens (*i.e.* whether they are present as oxide, hydroxyl or water) are difficult to detect.

The literature is particularly confused in regard to the existence of $x\text{PbO}\cdot\text{H}_2\text{O}$ phases with $x = 2.5$ and 3.0 since the published X-ray powder diffraction patterns are essentially identical (Todd & Parry, 1964; Oswald *et al.*, 1968; Glemser & Lin, 1971). In a single-crystal X-ray diffraction study of the analogous tin compounds, Howie & Moser (1968) dismissed the $x = 2.5$ phase as resulting from analytical error and proposed that the formula $3\text{SnO}\cdot\text{H}_2\text{O}$ is better written as $\text{Sn}_3\text{O}_2(\text{OH})_2$ to indicate the presence of hydroxyl groups rather than structural water molecules. The positions of the hydrogen atoms were not, however, located in this study, no list of Sn or O atomic coordinates was provided, and the R value was quoted as 0.16. Howie & Moser (1968) further proposed that the tin compound and the corresponding lead phase (also presumed to have the $x = 3$ composition) were isostructural because of the close similarity between their X-ray powder patterns.

These results are not in agreement with an infrared (IR) study of the $x = 3$ phase by Oswald *et al.* (1968), which indicated the presence of an HOH deformation vibration characteristic of structural water molecules. Moreover, a detailed chemical, X-ray, thermal and IR study by Glemser & Lin (1971) has confirmed the existence of the $x = 2.5$ phase and has shown that the compound is a hydroxide rather than a hydrate.

The present structure determination of the $x = 3$ phase was performed, not only in an attempt to resolve some of the confusion surrounding this material, but also as part of a general study of the role of hydrogen in the electrochemical activity of lead oxides in the positive plate of the lead-acid battery (Caulder, Murday & Simon, 1973; Hill, 1982, 1984; Hill & Madsen, 1984; Hill & Houchin, 1985; Hill, Jessel & Madsen, 1985). In particular, the lead hydrates and hydroxides have importance as possible intermediate phases during corrosion of the supportive and current-collecting lead grids in positive plates that have suffered alkalization

during deep discharge. Their study may also shed light on the mechanism of H incorporation into the PbO_2 structure and its role in the charge/discharge and corrosion reactions. Since the precise location of the hydrogen atoms is a key factor in the determination of unit-cell symmetry and structural formulae it was decided to undertake the structural studies with neutron diffraction data.

Experimental. A powder sample of $\text{Pb}_3\text{O}_2(\text{OH})_2$ was prepared by the slow addition of 2 L of concentrated (33%) ammonia solution to 1 L of 10% lead acetate with constant agitation. The pure white precipitate was washed repeatedly with distilled water, filtered and dried at 380 K.

Neutron diffraction data collected at 295 K on the high-resolution fixed-wavelength eight-counter diffractometer (HRPD) attached to the Australian Atomic Energy Commission research reactor HIFAR at Lucas Heights, New South Wales. This instrument (in an earlier single-counter configuration) has been described in detail by Howard, Ball, Davis & Elcombe (1983). Sample contained in a 16×50 mm spinning vanadium can, data recorded under monitor control at intervals of 0.05° between 15.04 and $159.99^\circ 2\theta$; for wavelength of 1.893 \AA this range of diffraction angles contains 221 unique Bragg reflections. μ determined by measuring the attenuation of the straight-through beam with and without a sample in the can. Since there is always a degree of uncertainty about the exact value of the wavelength in neutron diffraction studies, values of unit-cell parameters were obtained independently from X-ray powder diffraction data. These data were also used in early stages of structure analysis to obtain Pb atom coordinates, which were largely unaffected by neglect of the small X-ray scattering contribution from O. X-ray data were collected by back-pressing the sample into a standard aluminium holder mounted in a Philips PW 1050 diffractometer equipped with PW 1710 automatic step-scanning system and diffracted-beam curved graphite monochromator. Intensity measurements made at 295 K in intervals of 0.04° from 12 to $100^\circ 2\theta$, $\text{Cu K}\alpha$ radiation, 1° divergence and receiving slits and step counting time of 1.0 s .*

Differential scanning calorimetry carried out with a Setaram DSC III (Morano, 1978) using a Hewlett Packard 3421A Data Acquisition and Control Unit and a Hewlett Packard 85 microcomputer for data processing; the 82.7 mg sample was contained in a gold

* The lists of step-scan diffraction data and coefficients of the anisotropic thermal vibration parameters have been deposited with the British Library Lending Division as Supplementary Publication No. SUP 42049 (11 pp.). Copies may be obtained through The Executive Secretary, International Union of Crystallography, 5 Abbey Square, Chester CH1 2HU, England.

micro-boat, and heated under a stream of argon (5 ml min⁻¹) from 298 to 1100 K at 5 K min⁻¹. Another sample (23.1 mg) was subjected to differential thermal gravimetric analysis in a Stanton Redcroft STA-780 Thermal Analyser. The infrared spectrum was recorded in a KBr disc using a Digilab FTS-20 Fourier-transform Infrared Spectrometer; 50 scans were acquired in the region 4000–500 cm⁻¹ at a resolution of 4 cm⁻¹.

Structure determination and refinement. Least-squares structure refinements of both the neutron and X-ray diffraction data sets were performed with an extensively modified version of the Rietveld analysis program *DBW3.2* (Wiles & Young, 1981). The more important modifications to this program include the incorporation of a 2θ -variable pseudo-Voigt peak-shape function (Hill & Howard, 1985), a correction for sample absorption in the neutron beam (Hewat, 1979), and improvements to the method of extraction of 'observed' integrated peak intensities for the calculation of Fourier coefficients and Bragg agreement index. The scattering lengths used for Pb, O and H were 94.003, 58.03 and -37.409 fm², respectively, while the X-ray scattering factors were taken from *International Tables for X-ray Crystallography* (1974).

The background was defined by a four-parameter polynomial in $2\theta^m$, where m has values between 0 and 3, and was refined simultaneously with the unit cell, zero point, scale, peak width/shape/asymmetry and crystal structural parameters. The calculated peak intensity was distributed over 4.0 peak full-widths at half-maximum on either side of the peak centre. The function minimized in the least-squares procedure was $w_i(Y_{io} - Y_{ic})^2$, where Y_{io} and Y_{ic} are the observed and calculated intensities at each step i in the pattern, and $w_i = 1/Y_{io}$. Convergence was assumed to have been achieved when the parameter shifts in the final cycle of refinement were less than 20% of their associated e.s.d.'s.

Starting values for the coordinates of the two crystallographically distinct Pb atoms at $(x,y,0)$ and $(0,0,z)$ in space group $P4/mnc$ were estimated from the [001] projection presented by Howie & Moser (1968). These positions, along with the unit cell, background and other profile parameters, were refined with the X-ray data to yield conventional Rietveld analysis agreement indices (Young, Prince & Sparks, 1982) $R_{wp} = 0.191$, $R_B = 0.100$ and goodness of fit (g.o.f.) = 9.18. The resulting Pb coordinates were then fixed in a corresponding profile-only refinement of the neutron data ($R_{wp} = 0.114$, $R_B = 0.123$, g.o.f. = 13.56) and the positions of the O and 1/2 H atoms at (x,y,z) and $(x, x + 1/2, 1/4)$, respectively, were obtained from a Fourier difference synthesis. A full-matrix anisotropic thermal parameter refinement of the neutron data (14 profile and 23 structural parameters) then converged at $R_{wp} = 0.042$, $R_B = 0.016$ and g.o.f. = 1.892.

Table 1. *Fractional atomic coordinates and equivalent isotropic thermal parameters*

	x	y	z	$B_{eq}(\text{\AA}^2)^\dagger$
Pb(1)	0.1330 (4)*	0.2988 (4)	0.0012 (6)	1.8 (1)
Pb(2)	0.0	0.0	0.2779 (4)	1.7 (2)
O(1)	0.2624 (9)	0.0992 (10)	0.1716 (7)	2.0 (2)
O(2)	0.4230 (9)	0.3042 (8)	0.3744 (7)	1.8 (2)
H	0.3382 (18)	0.1516 (19)	0.2420 (21)	3.1 (5)

* Parenthesized figures here and elsewhere in the tables represent the e.s.d. in terms of the least significant figure to the left.

† B_{eq} is defined as $8\pi^2(\text{mean square radial displacement})/3$.

At this point the structure model consisted of isolated structural units of composition $\text{Pb}_6(\text{O}_1\text{H}_{1/2})_8$ and symmetry $4/m$ connected by disordered hydrogen bonds. This model is, however, clearly inadequate since the centrosymmetric space group $P4/mnc$ requires the hydrogen atom to be located on a twofold axis, equally shared between two O atoms in adjacent units separated by 2.8 Å. Examination of the anisotropic 'thermal' vibration parameters showed that the O atom (rather than H, as expected) was the only one with an unusually large ellipsoid ($B_{eq} = 5.0 \text{ \AA}^2$) and that the direction of maximum displacement was towards the H atom. The highest symmetry subgroup of $P4/mnc$ that permits the eight O atoms in the $\text{Pb}_6(\text{O}_1\text{H}_{1/2})_8$ cluster to be split into two sets of four, staggered around the corners of the cluster such that members of the same set do not face each other across the gap between clusters, is the non-centrosymmetric space group $P\bar{4}2_1c$. Anisotropic thermal vibration refinement (55 parameters) of the neutron data was, therefore, continued in $P\bar{4}2_1c$ with small initializing cooperative displacements applied to O(1) and O(2) towards and away from the H atom, respectively. Convergence was achieved at $R_{wp} = 0.0356$, $R_p = 0.0313$, $R_B = 0.0116$ and g.o.f. = 1.356, with smaller O-atom thermal parameters ($B_{eq} = 1.8$ and 2.0 \AA^2), much more sensible hydrogen-bond geometry, and a maximum level of residual nuclear density less than 6% of that of an O atom. The individual diffraction peak shapes were observed to vary linearly from 13.5 to 32.3% Lorentzian character in the range 15 to $160^\circ 2\theta$. A summary of the refined structural parameters is given in Table 1, and the corresponding observed, calculated and difference neutron diffraction profiles are presented in Fig. 1.

It was, of course, not possible to establish the absolute configuration of the structure using anomalous dispersion effects in the X-ray data since Friedel reflection pairs overlap in a powder pattern. However, a refinement of the X-ray data (wavelengths: $\text{Cu } K\alpha_1 = 1.54056$, $K\alpha_2 = 1.54439 \text{ \AA}$), with all atom positions fixed at their neutron-determined values, was used to obtain the unit-cell dimensions given in the *Abstract*. For these data the peaks varied from 49 to 73% Lorentzian character in the range $2\theta = 12\text{--}100^\circ$.

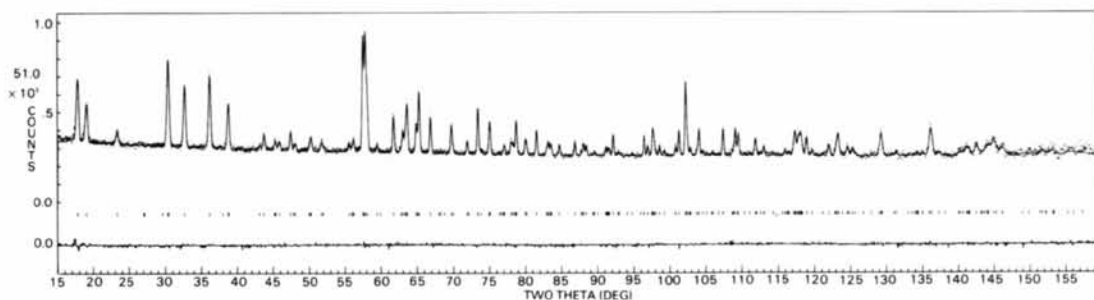


Fig. 1. Observed, calculated and 'difference' neutron powder diffraction profiles for $\text{Pb}_3\text{O}_2(\text{OH})_2$. The observed data are indicated by points and the calculated profile is the continuous line in the same field. The short vertical lines below the profiles represent the positions of all possible Bragg reflections, and the bottom curve is the value of $\text{sign}(\Delta)w\Delta^2$ at each step, where Δ is the difference between the observed and calculated intensity.

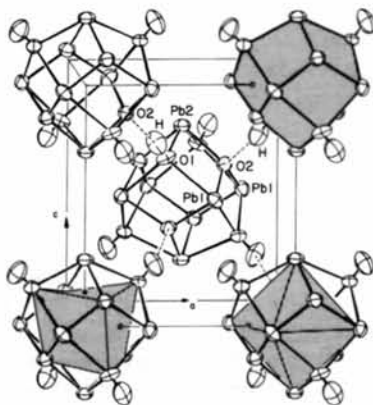


Fig. 2. Unit-cell diagram of the $\text{Pb}_3\text{O}_2(\text{OH})_2$ crystal structure viewed approximately down $[010]$; the clusters centred on the rear corners of the cell have been omitted for clarity. Thermal ellipsoids for all atoms represent 50% probability surfaces. Pb—O/O—H interactions and hydrogen bonds are shown as filled conical bonds and dashed lines, respectively. The opaque polyhedra included in the clusters at the unit-cell corners (1,1,1), (1,1,0) and (0,1,0) highlight the Pb_6O_8 dodecahedron, the suboctahedron of Pb atoms, and the distorted subcube of O atoms, respectively.

Table 2. Interatomic distances (Å) and angles ($^\circ$)

Pb(1)—O(2)	2.195 (8)	O(2)—O(1)	2.827 (9)	74.0 (2)
O(2)	2.205 (8)	O(1)	2.827 (9)	74.1 (3)
O(1)	2.480 (8)	O(1)	2.829 (10)	74.2 (2)
O(1)	2.483 (8)	O(1)	2.864 (10)	75.0 (3)
		O(2)	3.344 (11)	98.9 (3)
		O(1)—O(1)	4.513 (15)	130.8 (3)
Pb(2)—O(2)	2.206 (7) $\times 2$	O(2)—O(1)	2.829 (10)	74.4 (3) $\times 2$
O(1)	2.459 (7) $\times 2$	O(1)	2.864 (10)	75.5 (3) $\times 2$
		O(2)	3.376 (12)	99.9 (4)
		O(1)—O(1)	4.502 (15)	132.5 (3)
O(1)—H	0.988 (18)	H—Pb(2)	2.992 (14)	113.4 (11)
Pb(2)	2.459 (7)	Pb(1)	3.024 (18)	114.1 (11)
Pb(1)	2.480 (8)	Pb(1)	3.232 (18)	132.7 (10)
Pb(1)	2.483 (8)	Pb(1)—Pb(2)	3.679 (5)	96.2 (3)
		Pb(2)	3.694 (5)	96.8 (3)
		Pb(1)	3.710 (4)	96.8 (2)
		Pb(1)—Pb(2)	3.679 (5)	113.0 (3)
O(2)—Pb(1)	2.195 (8)	Pb(2)	3.694 (5)	114.2 (3)
Pb(1)	2.205 (8)	Pb(1)	3.710 (4)	115.0 (3)
Pb(2)	2.206 (7)			
Hydrogen bond				
H...O(2)	1.866 (18)	O(1)...O(2)	2.816 (9)	160.4 (14)

Discussion. The fundamental structural unit in $3\text{PbO}\cdot\text{H}_2\text{O}$ is a roughly spherical hollow dodecahedral cluster with composition $\text{Pb}_6\text{O}_4(\text{OH})_4$ and $\bar{4}$ symmetry located at the corners and centre of the unit cell (Fig. 2). This cluster has a diameter of 5.2 Å and may be visualized either as a slightly tetragonally distorted octahedron of Pb atoms (of mean edge length 3.69 Å) with all eight triangular faces capped by O, or as a heavily distorted cube of O atoms (of mean edge length 2.84 Å) with all six square faces capped by Pb (Fig. 2).

All O atoms in the cluster are coordinated to three Pb atoms, but the set of four O(1) are also bonded to H at a distance of 0.988 (18) Å (Table 2) and are, therefore, in roughly tetrahedral coordination. The O(2) atoms, on the other hand, are only bonded to H atoms at a distance of 1.866 (18) Å in adjacent clusters and remain in shallow trigonal pyramidal coordination. These hydrogen-bond lengths, together with the corresponding $\text{O}_d\cdots\text{O}_a$ distance and $\text{O}_d\cdots\text{H}\cdots\text{O}_a$ angle (Table 2), are close to the mean values determined by Chiari & Ferraris (1982) for crystalline hydrates studied by neutron diffraction. Based on electrostatic bond-strength-sum considerations (Brown & Wu, 1976) the Pb—O(1) bonds are expected, and observed, to be about 0.27 Å longer than the Pb—O(2) bonds (Table 2). As a result, the O(1) atom lies 1.253 (7) Å out of the plane of its three coordinated Pb atoms, whereas the O(2) atom lies only 0.546 (6) Å from its trigonal Pb plane.

The four equatorial Pb(1) and two apical Pb(2) atoms in the dodecahedral cluster are each bonded to two O(1) and two O(2) atoms in distorted square-pyramidal coordination. The plane of these four O atoms is 1.21 and 1.18 Å from Pb(1) and Pb(2), respectively, with the uncoordinated side of the Pb atom being occupied, presumably, by a lone pair of electrons with predominantly 6s character. Similar 'one-sided' coordination for divalent lead has been observed in both modifications of PbO, and a number of other more complex divalent lead salts (Sahl, 1970; Abel, 1973).

Pb(1) is surrounded by an approximately spherical array of seven other Pb atoms at distances of 3.7 to

3.9 Å (next nearest 4.7 Å), and Pb(2) has nine other Pb atoms at distances of 3.7 to 4.1 Å (next nearest >5 Å). All of these separations are significantly less than twice the value of 2.25 Å assigned to the van der Waals radius of a Pb atom lone-pair orbital (Dickens, 1965). Therefore, although the O(1)—H...O(2) hydrogen bonds represent the only direct link between the clusters, it is likely that van der Waals interactions between the lone pairs on Pb also exert control over the packing arrangement. Indeed, it may be competition between these van der Waals interactions and the steric requirements of the hydrogen bond that has resulted in the cluster at $(\frac{1}{2}, \frac{1}{2}, \frac{1}{2})$ in the unit cell being rotated by 41.4° about [001] with respect to the one at (0,0,0). No such rotation of the clusters has occurred parallel to [100] or [010] and, consequently, two lone-pair orbitals directly face each other across the 4.14 Å gap between Pb(2) atoms in the *c*-axis direction (Fig. 2). This 'head to head' contact between orbitals is, no doubt, the reason why the *c* axis is some 1.3 Å longer than *a* and *b*.

The structure refinement indicates, as suggested by Howie & Moser (1968), that the phase 3PbO.H₂O is more properly written as Pb₃O₂(OH)₂ since all of the H atoms are present as hydroxyl groups rather than as water molecules. The Fourier transform infrared spectrum in Fig. 3 is consistent with this observation (*cf.* Oswald *et al.*, 1968) in that there is only a very small peak at about 1650 cm⁻¹, which can be assigned to the ν₂ bending mode of a structural HOH group. In fact, this small peak probably arises from water chemisorbed on the particle surfaces (in agreement with the results of TGA experiments described below) and/or the KBr disc, or from a combination of lower-frequency fundamental vibrations. On the other hand, the large absorption band near 3200 cm⁻¹ is characteristic of the ν₁ and ν₃ stretching vibrations of a

hydroxyl group, shifted to lower frequencies (from the ideal value of 3700 cm⁻¹) by the effects of hydrogen bonding. Other absorption bands below 1500 cm⁻¹ probably arise from fundamental vibrations of Pb—O bonds in the Pb₆O₄(OH)₄ clusters.

Dehydration of Pb₃O₂(OH)₂ is accomplished in a single step between 410 and 460 K (Fig. 4), the residue eventually crystallizing as orthorhombic (yellow) PbO. For some samples, however, the total weight loss is up to 1 wt% higher than the theoretical value of 2.62 wt%, suggesting that they contain amorphous material of different composition and/or significant quantities of surface-adsorbed water.

Relevance to the lead-acid battery. If the Pb and O atoms in the Pb₆O₄(OH)₄ cluster are replaced by Ca and F, respectively, then it bears a striking resemblance to corresponding fragments in the unit cell of fluorite, CaF₂ (Bragg & Claringbull, 1965), the structure upon which tetragonal PbO (litharge) and the series of so-called 'intermediate' lead oxides are based (Byström, 1945; Anderson & Sterns, 1959). The structural connections between these compounds underline the importance of Pb₃O₂(OH)₂ in studies of the lead-acid battery since all are observed during corrosion of the current-collecting and supportive lead alloy grids in the positive plates. Moreover, if half of the O atoms are removed and the remaining Pb and O atoms are replaced by O and Sb, respectively, the cluster is essentially identical to the discrete Sb₂O₃ groups in senarmonite, Sb₂O₃ (Bragg & Claringbull, 1965), another phase that may be produced during oxidation of the Pb/Sb alloy grids. The phase Pb₃O₂(OH)₂ may, therefore, have a significant role to play as an intermediate compound during this corrosion process. The fact that H is an essential part of the structure further highlights the need for continued analysis of the role of H in lead-acid battery electrochemistry.

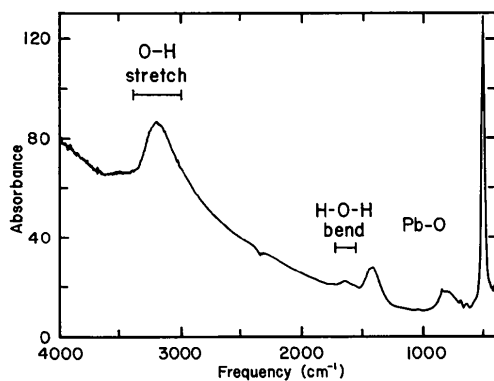


Fig. 3. Fourier transform infrared spectrum of Pb₃O₂(OH)₂.

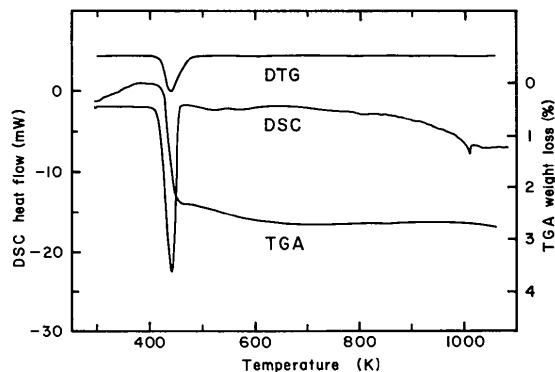


Fig. 4. Thermal analysis plots for Pb₃O₂(OH)₂, including differential scanning calorimetry (DSC), thermal gravimetric analysis (TGA), and differential thermal gravimetry (DTG) data.

The author is grateful to Mr A. J. Hruza of Ferro Corp. (Australia) for synthesizing the sample, to Messrs G. L. Corino and I. C. Madsen of the CSIRO Division of Mineral Chemistry for assistance with the collection of the thermo-analytical and X-ray diffraction data, respectively, and to Mr N. Brown of the Central Resource Laboratory, University of Tasmania for the FTIR measurements. The Australian Associated Smelters Pty Ltd is also thanked for financial assistance and permission to publish the results.

References

- ABEL, E. W. (1973). *Lead*. In *Comprehensive Inorganic Chemistry*, pp. 105–146. Oxford: Pergamon Press.
- ANDERSON, J. S. & STERNS, M. (1959). *J. Inorg. Nucl. Chem.* **11**, 272–285.
- BRAGG, L. & CLARINGBULL, G. F. (1965). *Crystal Structures of Minerals*. London: Bell & Sons.
- BROWN, I. D. & WU, K. K. (1976). *Acta Cryst.* **B32**, 1957–1959.
- BYSTRÖM, A. (1945). *Ark. Kemi Mineral. Geol.* **20A**, 1–31.
- CAULDER, S. M., MURDAY, J. S. & SIMON, A. C. (1973). *J. Electrochem. Soc.* **120**, 1515–1516.
- CHIARI, G. & FERRARIS, G. (1982). *Acta Cryst.* **B38**, 2331–2341.
- CLARK, G. L. & TYLER, W. P. (1939). *J. Am. Chem. Soc.* **61**, 58–65.
- DICKENS, B. (1965). *J. Inorg. Nucl. Chem.* **27**, 1495–1501.
- GLEMSER, O. & LIN, T.-P. (1971). *Z. Anorg. Allg. Chem.* **382**, 244–248.
- HEWAT, A. W. (1979). *Acta Cryst.* **A35**, 248.
- HILL, R. J. (1982). *Mater. Res. Bull.* **17**, 769–784.
- HILL, R. J. (1984). *J. Power Sources*, **11**, 19–32.
- HILL, R. J. & HOUGHIN, M. R. (1985). *Electrochim. Acta*, **30**. In the press.
- HILL, R. J. & HOWARD, C. J. (1985). *J. Appl. Cryst.* **18**, 173–180.
- HILL, R. J., JESSEL, A. M. & MADSEN, I. C. (1985). Proc. Lead-acid Battery Symposium, 166th Meeting of the Electrochem. Soc., New Orleans, 7–11 October.
- HILL, R. J. & MADSEN, I. C. (1984). *J. Electrochem. Soc.* **131**, 1486–1491.
- HOWARD, C. J., BALL, C. J., DAVIS, R. L. & ELCOMBE, M. M. (1983). *Aust. J. Phys.* **36**, 507–518.
- HOWIE, R. A. & MOSER, W. (1968). *Nature (London)*, **219**, 372–373.
- International Tables for X-ray Crystallography* (1974). Vol. IV. Birmingham: Kynoch Press. (Present distributor D. Reidel, Dordrecht.)
- MORANO, R. T. (1978). *Thermochim. Acta*, **26**, 27–37.
- OSWALD, H. R., GUNTER, J. R. & STAHLIN, W. (1968). *Helv. Chim. Acta*, **51**, 1389–1394.
- ROBIN, J. & THÉOLIER, A. (1956). *Bull. Soc. Chim. Fr.* pp. 680–681.
- SAHL, K. (1970). *Lead*. In *Handbook of Geochemistry*, pp. 82A1–6. Berlin: Springer-Verlag.
- TODD, G. & PARRY, E. (1964). *Nature (London)*, **202**, 386–387.
- TOLKACHEV, S. S., STROGANOV, E. V. & KOZINA, I. I. (1958). *Vestn. Leningr. Univ.* **16**, 134–139.
- WILES, D. B. & YOUNG, R. A. (1981). *J. Appl. Cryst.* **14**, 149–151.
- YOUNG, R. A., PRINCE, E. & SPARKS, R. A. (1982). *J. Appl. Cryst.* **15**, 357–359.

Acta Cryst. (1985). **C41**, 1003–1007

Structure of High-Pressure Phases of Barium Germanium Oxide, BaGe_2O_5

BY MITUKO OZIMA

Institute for Solid State Physics, University of Tokyo, Roppongi, Minato-ku, Tokyo 106, Japan

(Received 2 February 1985; accepted 11 March 1985)

Abstract. (i) BaGe_2O_5 , II: $M_r = 362.56$, monoclinic, $P2_1/a$, $a = 13.214$ (2), $b = 13.043$ (2), $c = 9.5501$ (8) Å, $\beta = 94.006$ (10)°, $V = 1642.0$ (4) Å³, $Z = 16$, $D_x = 5.86$ g cm⁻³, $\text{Ag } K\alpha$, $\lambda = 0.56087$ Å, $\mu = 130.9$ cm⁻¹, $F(000) = 2560$, $T = 300$ K, $R = 0.047$ for 2549 independent reflections. (ii) BaGe_2O_5 , III: orthorhombic, $Cmca$, $a = 5.5632$ (2), $b = 9.8711$ (6), $c = 14.3231$ (12) Å, $V = 786.56$ (10) Å³, $Z = 8$, $D_x = 6.12$ g cm⁻³, $\text{Ag } K\alpha$, $\mu = 136.7$ cm⁻¹, $F(000) = 1280$, $T = 300$ K, $R = 0.051$ for 535 independent reflections. BaGe_2O_5 , II (low-pressure and high-temperature phase) has three kinds of infinite chains of Ge polyhedra. One type (which is parallel to the b axis) is connected to another chain of the same type by the other two chains (which are parallel to the a axis) and two ladder-like sheets parallel to (201) and (201), respectively, are formed. BaGe_2O_5 , III (high-

pressure and low-temperature phase) has a sheet structure similar to that for the hexagonal perovskite-like compounds ABX_3 at high pressures. The increase in coordination number of Ba from BaGe_2O_5 , II to BaGe_2O_5 , III is accompanied by a large increase in density (4.4%).

Introduction. BaSi_2O_5 is known as the mineral sunbomite, which belongs to orthorhombic space group $Pmnb$ with cell dimensions $a = 7.6922$ (8), $b = 13.525$ (1), $c = 4.6336$ (5) Å [*Natl. Bur. Stand. (US) Monogr.*, 1976], which has a monoclinic high-temperature modification with $C2/c$, $a = 23.202$ (5), $b = 4.661$ (1), $c = 13.613$ (4) Å, $\beta = 97.54$ (2)° (Katscher, Bissert & Liebau, 1973) at atmospheric pressure. Both have undulating sheet structures which consist of Ge tetrahedra.